Supplemental Information

Supplementary Experimental Procedures.

Mouse lines

pTreH2BGFP, K5tTA, Sox9Cre, Sox9CreER, K14Cre, K14CreER, K15CrePGR, K5CreER, K14rtta, TetOCre, K18CreER, K19CreER, K14H2BGFP, K15eGFP, RosaLacZ, RosaYFP, RosaiDTR (Buch et al., 2005; Diamond et al., 2000; Morris et al., 2004; Soeda et al., 2010; Soriano, 1999; Tumbar et al., 2004; Van Keymeulen et al., 2011; Vasioukhin et al., 1999) were described previously.

Mouse Manipulations.

CreER was activated in adult mice by intraperitoneal (i.p.) injection with Tamoxifen (2mg/g in corn oil, Sigma) or topical application (~2 mg in ethanol) on paw pads. CrePGR was activated by i.p. injection with Mifipristone (RU486, 1.5mg/g in sesame oil, VWR) or topical application (~4mg in ethanol) on paw pads. For neonatal mice, subcutaneous injections were used.

For Ethynyldeoxyuridine (EdU, Invitrogen) labeling, adult mice were i.p. injected with EdU (1 μg/injection), and neonatal mice were intradermally (i.d.) injected with EdU (0.1 μg/injection). For cell ablation experiments, Rosa-iDTR mice were i.p. injected with DT (200 ng /injection, Sigma) daily for 4-8d. For paw pad wounding, mice were anesthetized with Ketamine/Xylazine (100mg/kg) and received preoperative subcutaneous Buprenorphine (0.1mg/kg). ~0.5mm incisions were administered to each paw (one front and one back foot). Exposed areas were then gently scraped with a #11 blade to create a scratch wound. Mice recovered in clean cages with paper bedding to prevent irritation or infection. Mice were monitored daily and sacrificed at specified times post wounding.

Immunofluorescence

Antibodies and dilutions used are as following: GFP (chicken, 1:1000, Abcam), SMA (rabbit, 1:200, Abcam), K18 (rabbit, 1:200, Fuchs lab), K19 (rat, 1:500, Developmental Studies Hybridoma Bank), K5 (rabbit, 1:500, Fuchs lab), K14 (rabbit, 1:500, Fuchs lab), Integrin-β1 (rat, 1:100, eBioscience,

Alexa647-conjugated), K8 (rat, 1:500, Developmental Studies Hybridoma Bank), Sca1 (rat, 1:100, eBioscience), Sox9 (rabbit, 1:1000, Fuchs lab), ATP1a1 (NKAα, rabbit, 1:8000, Abcam), ATP1b1 (rabbit, 1:50, SantaCruz), Fxyd2 (rabbit, 1:50, ProteinTech), Milk protein (rabbit, 1:20000, Nordic Immunology). EdU incorporation is detected by Click-It EdU Alexa Fluor 594 Imaging Kit (Invitrogen).

Image acquisition and processing

High-magnification images were acquired using inverted LSM780 laser scanning confocal microscope (Zeiss) through a 63x oil objective. RGB images were assembled using ImageJ software and Z-stacks were processed for 3D visualization using Imaris software (Bitplane).

Gene expression profiling

FACS purified samples were submitted to the Genomics Core Laboratory of the Memorial Sloan Kettering Cancer Center for RNA extraction, labeling, and hybridization to Affymetrix Mouse 430A_2 arrays. Statistical analyses were performed using R version 2.13.0, Bioconductor version 2.6 and Spotfire Decision Site 9.1.1 (Tibco, Somerville, MA). To compare sweat gland Mouse430A_2 array and mammary gland MOE430A array (Stingl et al., 2006), gene expression signals were normalized to the trimmed average of 500 in Affymetrix MAS 5.0 algorithm. MAS5 signals less than 2 were set to 2 before log2 transformation. For unsupervised clustering and principal component analysis, probe sets with MAS5 absent calls for all samples were excluded. Differential expression analysis was performed by limma with estimation of fold change and false discovery rate. Probeset lists were uploaded to the “Database for Annotation, Visualization and Integrated Discovery” (DAVID) v6.7 web tool to assess pathway enrichment.

Electron Microscopy

Foot pad samples were fixed in 2% glutaraldehyde, 4% PFA, and 2 mM $CaCl_2$ in 0.05 M sodium cacodylate buffer, pH 7.2, at room temperature for > 1 hr, postfixed in 1% osmium tetroxide, and processed for Epon embedding. Ultrathin sections (60–70 nm) were counterstained with uranyl

acetate and lead citrate. For immunogold labeling, foot pads were fixed in 4% formaldehyde, 0.05% glutaraldehyde in 0.05M sodium cacodylate buffer pH 7.2, Ca2+ 2 mM. Samples were embedded in LR White resin (London Resin Company, Ltd). Ultrathin sections were immunolabeled for GFP using an anti-GFP antibody (Invitrogen) followed by secondary antibody (goat anti-rabbit) coupled to 10nm gold particles (Aurion, The Netherlands). Images were taken with a transmission electron microscope (TEM) (Tecnai G2-12; FEI) equipped with a digital camera (model XR60; Advanced Microscopy Techniques, Corp.). For correlative light-electron microscopy of the grafts in mammary fat pad tissue, tissue was fixed in 4%PFA and embedded in OCT compound. 20 mm sections were imaged to identify GFP positive cells. OCT sections were subsequently fixed and processed for conventional transmission electron microscopy as indicated above. Consecutive semi-thin sections (800 nm) were cut and stained with toluidine and examined under bright-field microscope till the area of interest was localized. Consecutive ultrathin sections of this area were obtained and imaged by TEM.

Supplemental References

Buch, T., Heppner, F. L., Tertilt, C., Heinen, T. J., Kremer, M., Wunderlich, F. T., Jung, S., and Waisman, A. (2005). A Cre-inducible diphtheria toxin receptor mediates cell lineage ablation after toxin administration. Nat Methods *2*, 419-426.

Diamond, I., Owolabi, T., Marco, M., Lam, C., and Glick, A. (2000). Conditional gene expression in the epidermis of transgenic mice using the tetracycline-regulated transactivators tTA and rTA linked to the keratin 5 promoter. J Invest Dermatol *115*, 788-794.

Soeda, T., Deng, J. M., de Crombrugghe, B., Behringer, R. R., Nakamura, T., and Akiyama, H. (2010). Sox9-expressing precursors are the cellular origin of the cruciate ligament of the knee joint and the limb tendons. Genesis.

Soriano, P. (1999). Generalized lacZ expression with the ROSA26 Cre reporter strain. Nat Genet *21*, 70-71.

Supplemental Figure Legends

Figure S1. Proliferation occurs during the morphogenesis of sweat gland/duct, related to Figure 1.

(A) Immunofluorescent images of developing or mature sweat duct/gland at stages as indicated. H2BGFP is expressed under K5 promoter and EdU was injected 4hr before harvesting the tissues. Scale bar, 10μm.

(B) Representative immunofluorescent images of EdU pulse-chase experiments as indicated. Arrows, EdUhi cells. Arrowheads, EdU^{lo} cells. White, myoepithelial cells. Yellow, luminal cells. Scale bars, 10μm.

Figure S2. Adult sweat glands do not undergo extensive turnover during normal homeostasis, related to Figure 2.

(A) Representative image of a sweat duct from an adult mouse that was injected with EdU daily for 3 days, showing basal cells of the sweat ducts are highly proliferative during adult homeostasis. Dashed lines mark the basement membrane. Scale bar, 10μm.

(B) Representative images of the sweat glands from adult mice that were injected with EdU daily for 2 wks, showing rare cases of proliferation occurred in both myoepithelial cells (top) and luminal cells (bottom). Scale bars, 10μm.

(C) K5CreER/RosaYFP, (D) K18CreER/RosaYFP, (F) K19CreER/RosaYFP mice were induced at P28 (for 1-5 days as specified) and their sweat glands were examined 1 wk and 8 wk (or 10, 12 wks as specified in the images) after Cre induction. Note that results obtained from 1 wk and at least 8 wks after induction are similar, as shown in graphs at right.

Figure S3. Luminal cells in the sweat glands do not participate epidermal wound repair, related to Figure 3.

Paw pads from non-wounded, 3 days and 2 weeks post-wound K15CrePGR/RosaLacZ mice (from left to right). Cells in blue (LacZ+) label luminal cells in the glands. Note the absence of LacZ+ cells in the repaired epidermis. Scale bar, 50 μm.

Figure S4. Luminal cells in the gland proliferate in response to luminal apoptosis arising from glandular injury, related to Figure 4.

(A-C) Ultrastructure analysis of the sweat glands before and after 8 days of diphtheria toxin (DT) treatment. Luminal cells are false-colored in purple, myoepithelial cells in green.

(A) Before DT treatment (DT0d), a cross-sectioned gland exhibit a luminal space (Lumen) surrounded by intact luminal cells (Lum). A myoepithelial (Myo) cell is shown at the periphery of the gland. Scale bar, 2μm, valid for (B) and (C).

(B) After 8 days of DT treatment (DT8d), most luminal spaces have collapsed and are no longer visible in the cross-sectioned ducts. While myoepithelial cells exhibit a normal ultrastructure, luminal cells show abnormal organelles in their cytoplasm (boxed areas are enlarged in B' and B''). (B') A healthy intact myoepithelial cell is shown beside a luminal cell with numerous apoptotic bodies in its cytoplasm. Ap, apoptotic bodies, as pointed by arrows. Scale bar, 1μm. (B'') A portion of cytoplasm of a normal myoepithelial cells is shown contiguous to the cytoplasm of a luminal cell containing apoptotic bodies. Scale bar, 500nm.

(C) After 8 days of DT treatment, a luminal cell in mitosis (Mi, outlined by dotted line) can be detected in the gland, in proximity to a myoepithelial cell and other luminal cells.

Figure S5.Validation of FACS sorting strategy and analyses, related Figure 6.

(A) pTreH2BGFP/K5tTA mouse treated with doxy for 6 weeks. Image taken from Figure 1D showing GFP+ label-retaining cells are restricted to sweat gland myoepithelial cells. FACS scheme shows GFP^{hi} cells are exclusively $\beta1^{hi}$Sca1- (indicating myoepithelial cells, Myo); while GFP^{lo} population

consist of β1^{med}Sca1- and β1^{med}Sca1+, representing luminal cells (Lum) and cells in the sweat duct (SD). Cytospin analyses at right confirming the identity of Myo and Lum by SMA and K18 staining, respectively.

(B) Image of a paw pad from K15-eGFP mouse is shown. Note that GFP+ cells are restricted to the glands. FACS scheme taking GFP+ population shows exclusively β1^{med}Sca1-, indicating Lum; while β1^{med}Sca1+ (SD) and β1^{hi}Sca1- (CD-Myo) are found in GFP- population. Cytospin analyses of SMA, K18, and K5 confirmed their identity.

(C) FACS analysis for K14Cre/RosaYFP mice, showing Myo, Lum, and SD are all YFP+. This result is consistent with Figure 2A.

(D) FACS analysis for P23 adult Sox9CreER/RosaYFP mouse induced at P1 and P2, showing YFP+ population consists of Myo, Lum, and SD. This result is consistent with Figure 2C.

(E) FACS analysis for P28 adult K15CrePGR/RosaYFP mouse induced at P5-7, showing YFP+ cells are exclusively Lum. This result is consistent with Figure 2E.

(F) FACS analysis of K15CrePGR/RosaYFP mouse induced at adult stage for 4 days, showing YFP+ population is exclusively Lum. This result supported the experiment in Figure 4A and 4B, where K15CrePGR was also used. Note that Lum is exclusively induced after Cre induction.

(G) FACS analysis of K14CreER/RosaYFP mouse induced at adult stage for 4 days, showing YFP+ population is exclusively Myo. Note that the induction efficiency of this mouse line is very low, therefore, only a small percentage of myoepithelial cells are YFP+. This result supported the experiment in Figure 4C, where K14CreER was used. Note only Myo is induced after Cre induction, and not SD.

Figure S6. Purified sweat gland and sweat duct cells generate *de novo* sweat gland-like structure upon transplantation into virgin mammary fat pads and shoulder fat pads, related to Figure 7.

(A) EdU labeling denotes proliferation within the glandular structure. Scale bar, 10 μm, also valid for (B) and (C).

(B) 4 focal planes from the z-stack images for RosaYFP myoepithelial cell graft, showing a coiled-duct like structure. Yellow dashed lines mark the tiny lumen or channel through compartment A-D. A blend 3D projection of the z-stack is shown on the right, demonstrating the connectivity between the compartments.

(C) Immunoflourescent confocal images of glandular structure formed from K14H2BGFP sweat duct basal call and sweat gland myoepithelial cells after grafted into mouse shoulder fat pad for 8wks. Note all GFP+ cells are positive for SMA and localized peripherally, K18+ cells are GFP-, and the entire structure exhibit ATP1a1 (sweat gland specific marker) expression. No significant difference observed in glandular colonies formed from these two cell types.

Table S1.

(A) Examples of sweat gland myoepithelial signature genes. DAVID functional annotation of genes up-regulated in sweat gland myoepithelial cells, with at least 2 fold up against the rest of populations in the sweat gland/duct combined. False discovery rate (FDR) < 0.2.

(B) Examples of sweat gland luminal signature genes. DAVID functional annotation of genes up-regulated in sweat gland luminal cells with at least 2 fold up against the rest of populations in the sweat gland/duct combined. FDR < 0.2.

Table S2.

(A) DAVID functional annotation for example key genes that are up-regulated in myoepithelial cells of both sweat gland and mammary gland.

(B) DAVID functional annotation for example key genes that are up-regulated in luminal cells of both sweat gland and mammary gland.

Supplementary Figure 1. Proliferation occurs during the morphogenesis of sweat gland/duct, related to Figure 1.

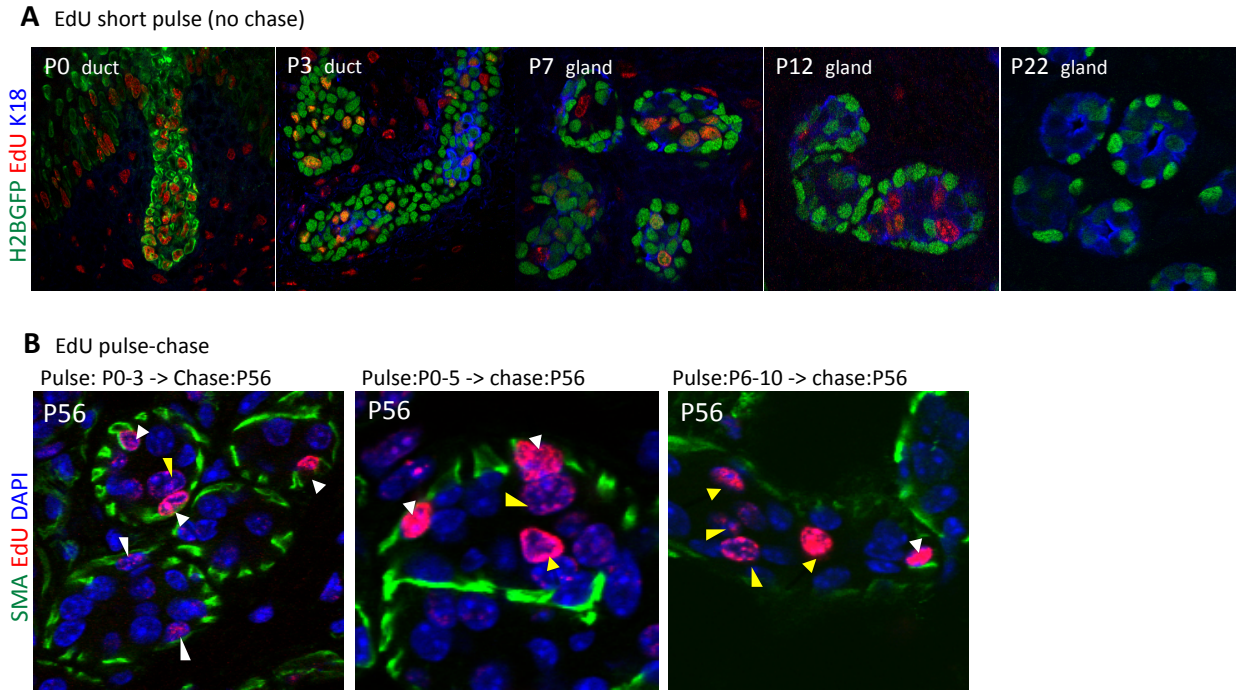

Supplementary Figure 2. Adult sweat glands do not undergo extensive turnover during normal homeostasis, related to Figure 2.

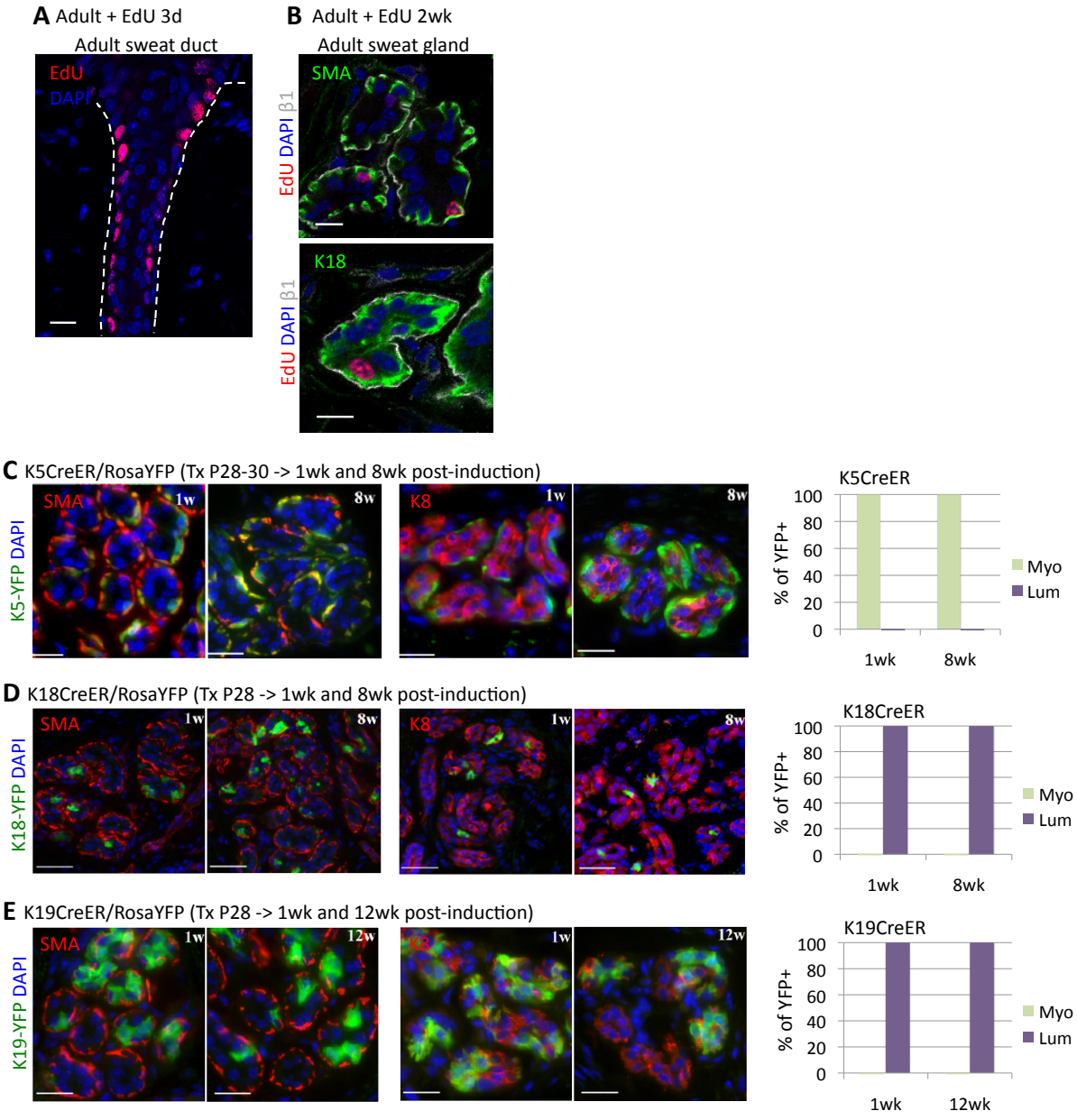

Supplemental Figure 3

.

Supplementary Figure 3. Luminal cells in the sweat glands do not participate epidermal wound repair, related to Figure 3.

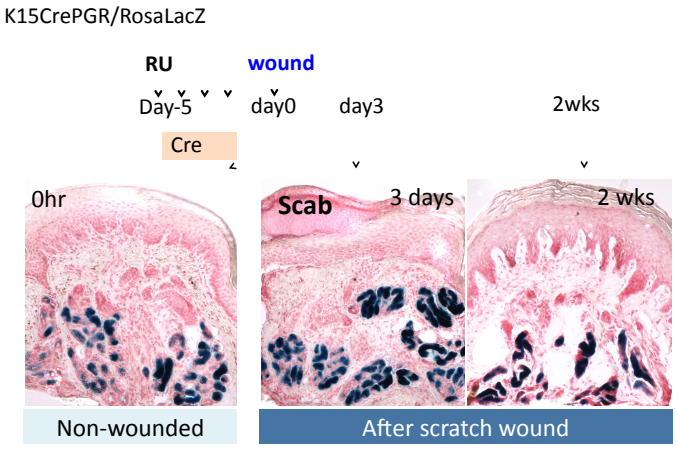

Supplemental Figure 4

Supplementary Figure 4. Luminal cells in the gland proliferate in response to luminal apoptosis arising from glandular injury, related to Figure 4.

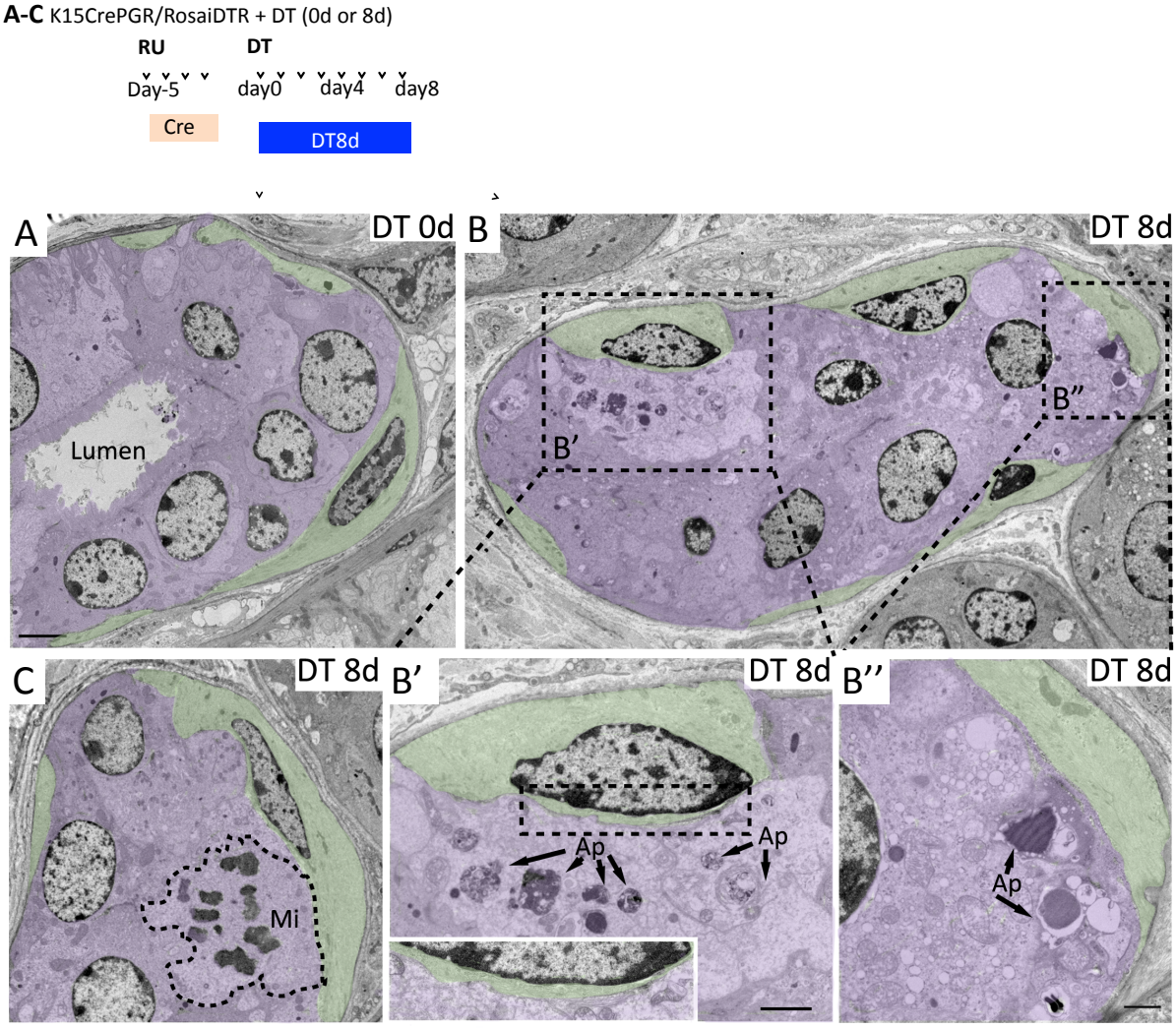

Supplemental Figure 5

Supplementary Figure 5. Validation of FACS sorting strategy and analyses, related to Figure 6.

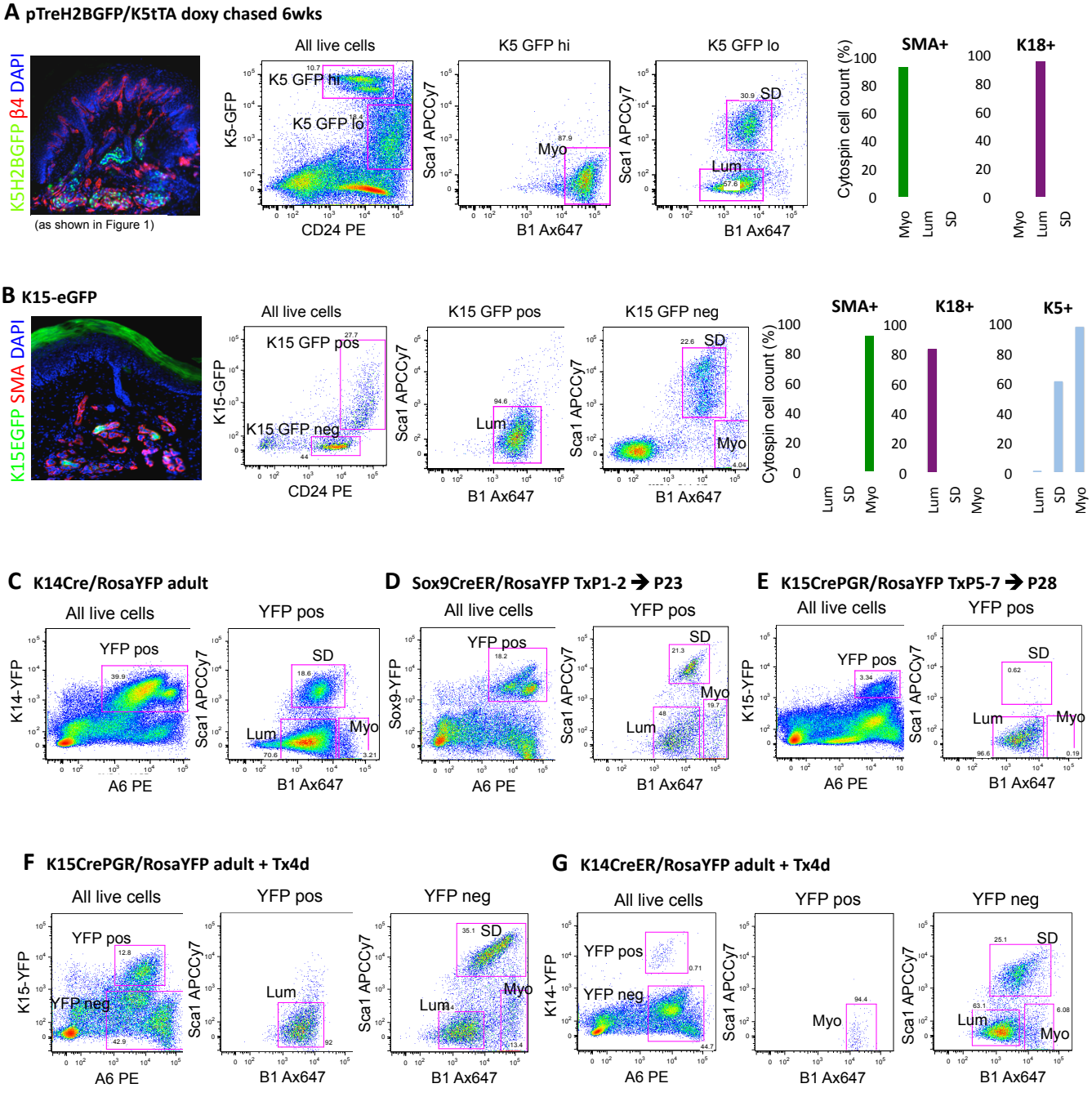

Supplementary Figure 6. Purified sweat gland and sweat duct cells generate *de novo* sweat gland-like structures upon transplantation into virgin mammary fat pads and shoulder fat pads, related to Figure 7.